

ROAD JUNCTION EXTRACTION FROM HIGH-RESOLUTION AERIAL IMAGERY

MEHDI RAVANBAKSH (ravanbakhsh@ipi.uni-hannover.de)

CHRISTIAN HEIPKE (heipke@ipi.uni-hannover.de)

KIAN PAKZAD (pakzad@ipi.uni-hannover.de)

Leibniz Universität Hannover, Germany

(Extended version of a paper submitted to the ISPRS conference “Photogrammetric Image Analysis—PIA 2007”, held at Technische Universität München, Germany, 19th to 21st September 2007)

Abstract

Road junctions are important components of a road network. However, they are usually not explicitly modelled in existing road extraction approaches. In this research, road junctions are modelled in detail as area objects and an approach is proposed for their automatic extraction through the use of an existing geospatial database. Prior knowledge derived from a topographic geospatial database is used to facilitate the extraction. A new snake-based approach is proposed that makes use of the “ziplock snake” concept and whose external force is a combination of the gradient vector flow (GVF) force and the balloon force in order to delineate the junction border. Road arm extraction results provide fixed boundary conditions for the proposed snake. The approach was tested using aerial black-and-white Digital Mapping Camera (DMC) ortho-images of 0.1 m ground resolution taken from suburban and rural areas. The results obtained demonstrate the validity of this approach.

KEYWORDS: balloon snake, geospatial database, gradient vector flow, high resolution, road junction, ziplock snake

INTRODUCTION

THE NEED FOR ACCURATE geospatial databases and their automatic updating increases rapidly. Geospatial databases contain various man-made objects among which roads are of special importance as they are used in a variety of applications such as car navigation, transport and fire services. As their extraction from images is costly and time-consuming, automation is seen as a promising solution to this dilemma. The problem for automatic data extraction lies mostly in the complex content of aerial images. To ease the automation of an image interpretation task, prior information can be used (de Gunst and Vosselman, 1997; Boichis et al., 1998, 2000; Gerke, 2006). This often includes data from an external geospatial database. Road junctions are important components of a road network and if modelled well can improve the quality of road network extraction. Road junctions in road network extraction systems have mainly been modelled as point objects at which three or more road segments meet. The junction position in such systems is computed by simple extension of neighbouring road segments. This kind of



FIG. 1. Superimposition of vector data on a high-resolution aerial image.

modelling does not always reflect the required degree of detail. In Fig. 1, vector data is superimposed on a sample image to describe the problem. At the given image resolution, the junction centre covers an area including a few small traffic islands, so the image provides enough information to consider the junction as an area object. In order to capture this degree of detail, a detailed modelling of junctions is needed in the data acquisition step.

The approach for road junction extraction suggested in this paper (for earlier work see Ravanbakhsh et al., 2007) uses an existing geospatial database as input and leads to the extraction of refined road junction data. In the next section, related work in this area is described. Then, the object model is introduced. The extraction strategy is described in detail in the following section. In the subsequent section, results from the implementation of the proposed approach using black-and-white aerial ortho-images with a ground resolution of 0.1 m are presented and discussed, together with their quality evaluation. The paper concludes with a summary and an outlook.

RELATED WORK

Although road junctions are important elements for the reconstruction of a road network, there are only a few approaches which are dedicated to the extraction of junctions. Most of the existing approaches initially concentrate on road extraction to create the road network. Subsequently, the extraction of road junctions is achieved by perceptual grouping of road hypotheses. In such approaches, junctions are regarded as point objects (Hinz et al., 1999; Wiedemann, 2002; Zhang, 2003).

In contrast, there are some approaches which treat junctions as planar objects (Laptev, 1997; Mayer et al., 1998; Laptev et al., 2000; Gautama et al., 2004). In Gautama et al. (2004) a differential ridge detector in combination with a region-growing operator is used to detect junctions and in Laptev (1997), Mayer et al. (1998) and Laptev et al. (2000) a snake model is used to delineate junctions.

Snakes, also called parametric active contours (Kass et al., 1988), are especially useful for delineating objects that are hard to model with rigid geometric primitives. Since the borders of road junctions are of diverse shapes including various degrees of curvature, snakes are well suited for this task. Snakes are polygonal curves associated with an objective function that combines an image term, external energy, measuring the image force (for example, the edge strength) and a regularisation term, internal energy, minimising the tension and curvature of the polygon. The curve is deformed so as to optimise the objective function iteratively.

Traditional snakes are sensitive to noise and need a precise initialisation. Since junction borders have various degrees of curvature a close initialisation often cannot be provided. As a result, traditional snakes can easily get stuck in an undesirable local minimum. To overcome these limitations, the ziplock snake model was proposed (Neuenschwander et al., 1997). Ziplock snakes need far less initialisation effort and are less affected by the shrinking effect from the internal energy term (Wang and Li, 2003). Furthermore, the computational process is more robust because the active part whose energy is minimised is always quite close to the contour being extracted. This modified snake model can detect image features even if the initialisation is far away from the solution. However, it can still become confused in the presence of disturbances. As a result, user intervention is necessary to fix the problem.

In Laptev (1997), a method based on the ziplock snake is presented to detect road junctions. The initial snake is supplied by two far endpoints sharing the same junction border. These endpoints are previously obtained by a snake-based approach designed to extract adjacent crossing roads. Since initial curves are straight and often lie outside the junction area, junction borders must contain sufficient contrast to prevent leakages to the surrounding area. In Mayer et al. (1998) and Laptev et al. (2000), instead of ziplock snakes, a closed snake is initialised inside the central area of the junction and expanded until it delineates the junction borders. However, various types of features which often are present inside the junction, such as cars, traffic islands and road markings, can block the snake's movement. Furthermore, problems may occur where tree shadows occlude junction borders. Since expanding snakes can pass over weak junction borders, sufficient contrast of the desired boundaries is a necessary precondition for a successful delineation.

There are also some methods which exclusively deal with junctions. Barsi et al. (2002) present a road junction operator developed for high-resolution black-and-white images. The operator uses a feed-forward neural network applied to a running window to decide whether it contains a road junction. The drawback of the system is the high level of false alarms. Wiedemann (2002) uses a method to improve the quality of the junction extraction which resulted from the approach presented in Hinz et al. (1999). In Wiedemann (2002), several internal and external evaluation measures are used for the combination of connected roads. The solution with the largest evaluation score is regarded as the correct one for the junction. In Boichis et al. (1998, 2000) a knowledge-based system for the extraction of road junctions is presented. Junctions are classified into four classes and each class is modelled separately. The information derived from an external database is used to generate hypotheses for the junction shape and for main and secondary roads. A drawback of this approach is that image information is not exploited for the selection of main and secondary roads.

MODEL OF THE ROAD JUNCTION

Road Junction Classes

For road traffic, various kinds of junctions have been designed. Different types of junctions have different properties and construction specifications. Junctions are classified into three main classes: simple, complex and motorway. Simple junctions contain three or more road arms without traffic islands in the centre. In contrast, complex junctions do contain traffic islands in the centre. A road model for simple and complex junctions complies with the classic road model in which roads are defined as quadrilateral objects with parallel edges and a constant width; however, in the complex class, the width of roads might increase when approaching the road junction. The main difference between motorway junctions and the two other classes is that crossing roads do not have the same height. In other words, simple and

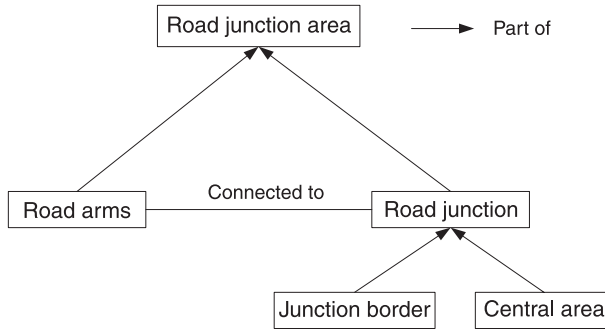


FIG. 2. Road junction model.

complex junctions are defined in two-dimensional space, whereas motorway junctions are defined in three-dimensional space. Roundabouts include the same properties as complex junctions with the exception that their central island is very large. Therefore, they are regarded as a subclass of complex junctions. In this paper, only simple junctions are considered, excluding complex and motorway junctions.

Road Junction Model

The conceptual model of simple road junctions is represented and described in Fig. 2.

According to the model, a junction area is composed of two parts: the junction itself and the road arms. A road arm is a long straight road segment connected to the junction. The junction, where road arms are connected, is composed of the junction border and its central area. The road arm is defined in terms of geometry and radiometry as follows:

- (1) Geometry: a road arm is a rectilinear object which is represented as a ribbon with a constant width and two parallel edges.
- (2) Radiometry: a road arm is considered to be a homogeneous region with a high contrast to its surroundings. The absolute brightness depends on the surface material.

Disturbances such as occlusions and shadows are not explicitly included in the model.

EXTRACTION APPROACH

The strategy consists of three steps (Fig. 3). First, the topographic geospatial database is analysed and different types of parameters for road junctions and crossing roads are derived. Second, road arms are extracted from high-resolution aerial ortho-imagery using prior information obtained from the previous step. Finally, the road junction is reconstructed using a snake-based method. The output result is the junction border connected to the road arms.

Pre-analysis of Geospatial Database

The topographic geospatial database used here contains explicit geometrical and implicit topological and radiometric information about road junctions. Topological information determines the number of roads connected to the junction centre and geometrical information provides the approximate location of the junction and the direction and width of the connected roads. A road junction in the geospatial database is composed of a centre point at which a few

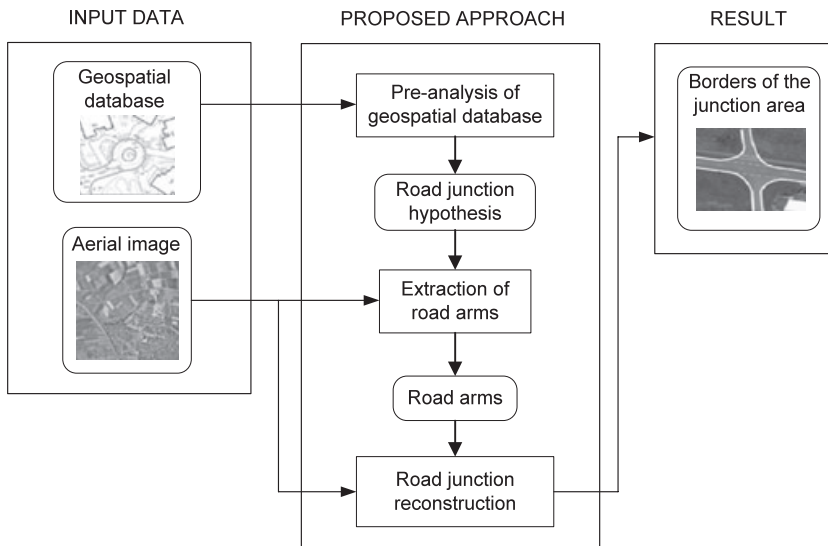


FIG. 3. Organisation of the proposed approach.

lines or polylines meet. Road directions are computed using vector coordinates of lines. In the road extraction step, geometrical and topological information is used to construct road segments. Furthermore, the database is assumed to contain information about the road surface material, from which radiometric properties of roads can be derived.

Extraction of Road Arms

Roads can be bent in different ways, for instance, in a simple curved form, a serpentine curve or in a state with changing width. However, in the area close to the junction centre they are mostly straight, partly because of traffic safety regulations. This observation leads to the decision to extract long and straight road segments near the junction centre, described here as road arms (Fig. 4). Since in high-resolution images (Fig. 5(a)) the surface of a road does not necessarily appear as a homogeneous region and many edges are usually detected around road sides, the process is performed at a somewhat reduced resolution equivalent to 0.2 m on the ground and the results are transferred back into the original image. In order to apply the geometrical part of the road model, edges are extracted from the image using the Deriche edge detector. It should be noted that throughout this paper the word “edge” is reserved explicitly for topological and image processing contexts, to avoid any confusion the physical edge of a road is described as “side” or “border”.

Subsequently, a thinning operation is applied, yielding edges 1 pixel wide. The edges are approximated by polygons to facilitate further processing (Fig. 5(b)). The result of this step is called *edge segments*. They are grouped on the basis of two geometrical criteria: parallelism and overlap. As roads are defined as homogeneous surfaces, radiometric homogeneity is subsequently checked for quadrilateral areas within the parallel and overlapping edge segments. This means the variance within each area must be smaller than a predefined threshold. Threshold values for all parameters used are specified in Table I, see Result section. As a result of these two steps, irrelevant edge segments are eliminated (Fig. 5(c)). Computed edge segment information includes image coordinates of endpoints, length and direction. The

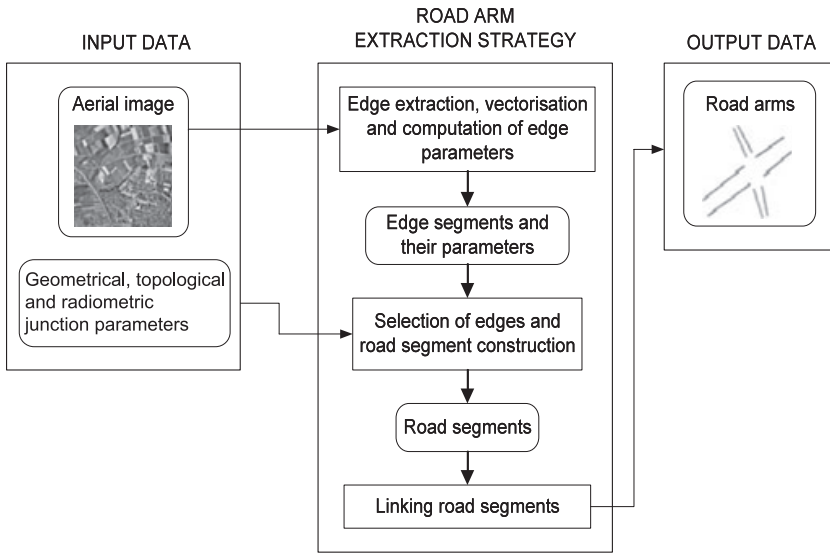


FIG. 4. Road arm extraction.

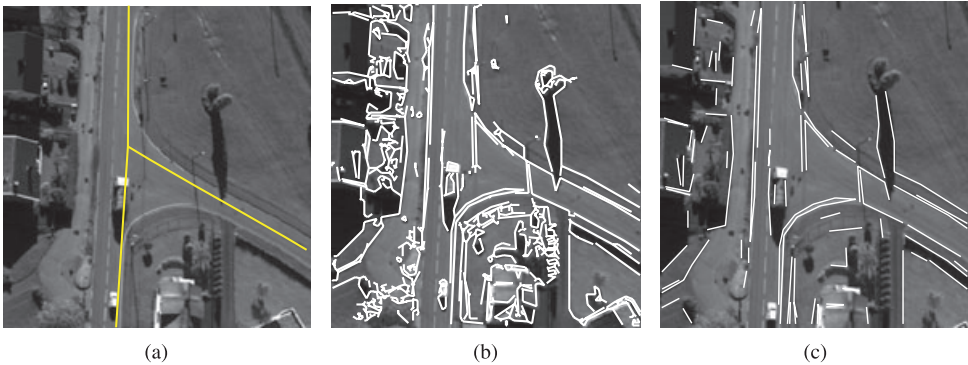


FIG. 5. (a) Vector data overlaid on the clipped image. (b) Edge segments. (c) Grouped edge segments.

direction is calculated so that it lies within the range of 0 to 180° , that is, all direction angles are projected to a half circle. These parameters are used later for road segment construction.

Edge segments are then grouped based on the direction of connected roads from the geospatial database. The number of groups corresponds to the number of connected roads (Fig. 6(a)). Since road directions derived from the geospatial database are regarded as reference directions, each group should contain parallel edge segments having a direction similar to their reference direction. It is noted that the difference of direction between edge segments in each group must be below a predefined threshold. Next, the width between two edge segment candidates is checked. A prerequisite for this step is that two candidates must have opposite image gradient vectors perpendicular to the edge direction (anti-parallelism condition) (Fig. 6(b)). Next, radiometric properties of the resulting road segments are investigated.

TABLE I. Road model parameters and associated thresholds.

Road model parameters	Threshold
Road width: the width of extracted road segments (W_E) must fall within the range defined by the road width derived from the geospatial database (W_R).	$W_R + T_w > W_E > W_R - T_w, T_w = 2 \text{ m}$ where T_w denotes the width tolerance
Parallelism: road segments are generated by parallel edge segments (width consistency condition). The difference between the direction of each group of edge segments (dir_E) and the reference direction (dir_R) must be below a predefined threshold (Th_{dir}).	$ dir_E - dir_R < Th_{dir},$ $Th_{dir} = 0.2618 \text{ radians or } 15 \text{ degrees}$
Mean grey value of road segments (GV) must fall within the grey value range defined by the reference grey value GV_R estimated from the geospatial database.	$GV_R + T_{gv} > GV > GV_R - T_{gv}, T_{gv} = 40$ where T_{gv} denotes the grey value tolerance
Standard deviation of road segments' grey values σ_{gv} must be below a predefined threshold (Th_σ).	$\sigma_{gv} < Th_\sigma,$ $Th_\sigma = 40$

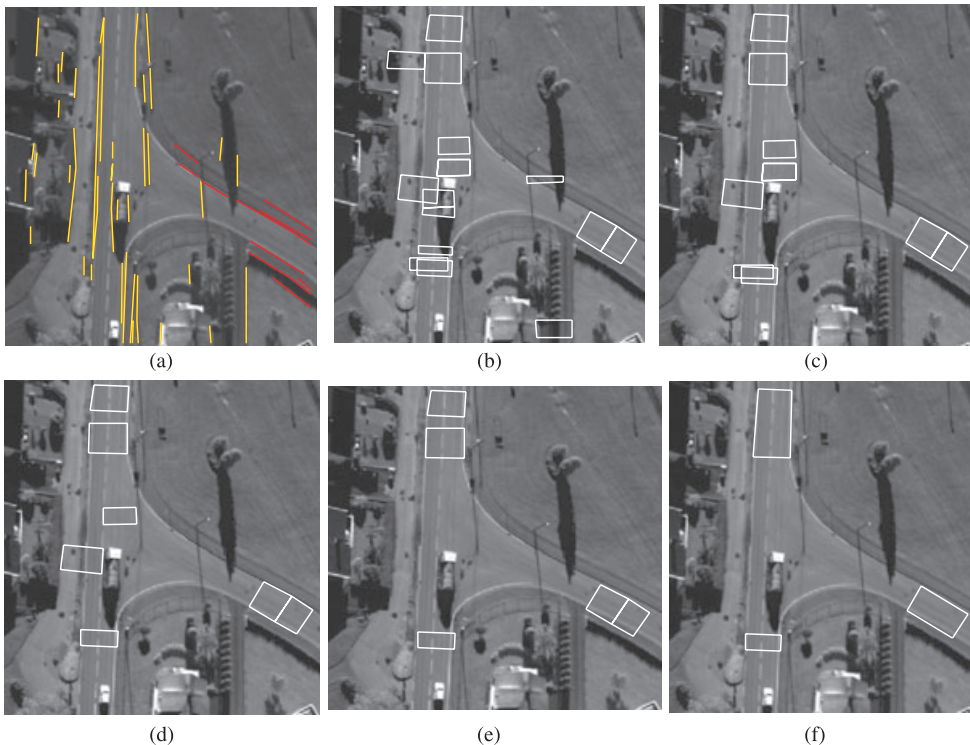


FIG. 6. (a) Two groups of edge segments in red and yellow. Yellow edge segments contain two groups since related roads are collinear. (b) The resulting road segments after applying geometric anti-parallelism and width features of the road model. (c) Result obtained after applying the radiometric brightness property. (d) Resulting road segments after removing overlapping road segments. (e) Verified road segments. (f) Extracted road arms.

According to the radiometric road model, the area between two road edges should be bright. This means the mean grey value within each area must fall into a predefined range.

As is shown in Fig. 6(c), some resulting road segments from this stage might overlap. It was decided to select the longer segment in each group of overlapping road segments as shorter segments are more likely to be generated from edge fragments of features close to road sides (Fig. 6(d)). The remaining road segments are verified using lane markings if any are found in the image (the line extraction method of Steger, 1998, is used for this task), otherwise road centrelines extracted in the image with a reduced resolution of 2 m (Steger, 1998) are used for the verification. Road segments are verified if lane lines or road centrelines are located within the road segments (Heipke et al., 1995) (Fig. 6(e)).

Although so far groups of road segments have been extracted, what is needed is one road arm per group. To achieve this purpose, road segments within each group are linked. Linking between road segments is carried out when they are collinear and have a similar width (Fig. 6(f)). Next, the orientation of each resulting road arm is investigated with the aim of deciding which endpoint faces the junction. This information could be taken from the geospatial database, but in order to be more independent, the distance between the endpoints of pairs of road arms is computed, and subsequently the endpoints sharing the shortest distance selected.

Road Junction Reconstruction

Based on the discussion in the second section it was decided to use ziplock snakes for reconstructing road junctions. Ziplock snakes are briefly described here to provide a basis to introduce the approach used. A ziplock snake consists of two parts: an active part and a passive part (Fig. 7(a)). The active part is further divided into two segments, indicated as head and tail, respectively. The active and the passive part of the ziplock snake are separated by moving force boundaries. Unlike the procedure for a traditional snake, the external force derived from the image is turned on only for the active parts. Thus, the movement of passive vertices is not

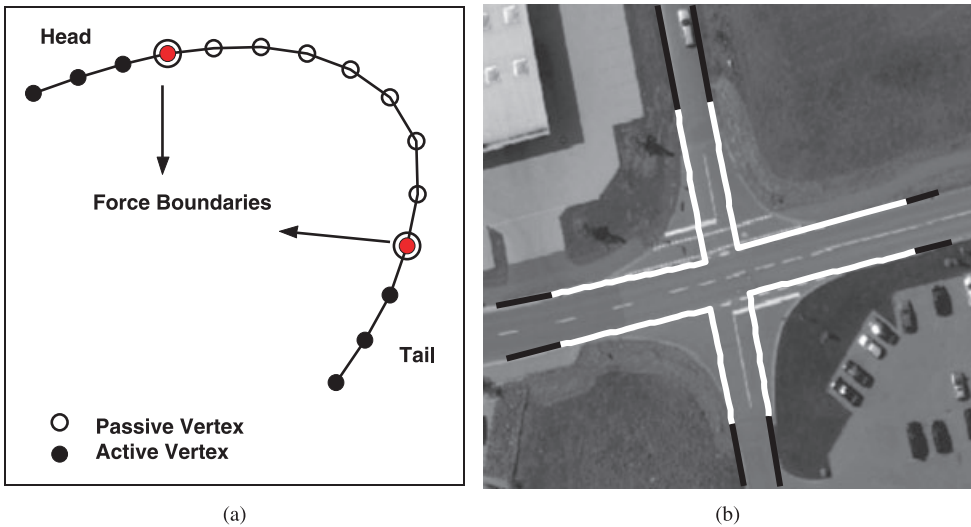


FIG. 7. (a) Ziplock snake during optimisation. (b) Global initialisation. Intersection lines in white are defined by two close endpoints and the intersection point of their respective road sides.



FIG. 8. Ziplock snake optimisation using a traditional force field as an external force. White curves are the result of snake optimisation. Black lines are the extracted road arms. Since the capture range of the external force field is small, the iterations are stopped near the initial positions.

affected by any image forces. Starting from two short pieces, the active part is iteratively optimised to image features, and the force boundaries are progressively moved towards the centre of the snake. Each time that the force boundaries are moved, the passive part is re-interpolated using the position and direction of the end vertices of the two active segments. Optimisation is stopped when force boundaries meet each other. The external force used in the ziplock snake is called *traditional force field*.

In the present approach, a global initialisation is introduced to ensure that snake vertices are distributed along the entire object boundary. The global initialisation is provided by pairs of lines, each of which is defined by close endpoints and the intersection point of their related road sides (Fig. 7(b)). These lines are called *intersection lines*. They are divided up into equidistant vertices surrounding the road junction border which is usually curved.

The ziplock snake method was tested on several samples (Fig. 8). As opposed to low-resolution images where the road surface appears homogeneous, in high-resolution images, the disturbances mentioned may destabilise the ziplock's active vertices. As a result, no convergence may occur, or the snake may get trapped near the initial position. In order to overcome this problem, an external force with a large capture range is advantageous. The gradient vector flow (GVF) field (Xu and Prince, 1997) is an example of such an external force, and is used in the present approach. A short review of GVF is provided here because according to the authors' knowledge this approach has not yet appeared in the photogrammetric literature.

The GVF field was proposed to address two issues: a poor convergence to concave regions and problems associated with the initialisation. It is computed as a spatial diffusion of the gradient of an edge map derived from the image. This computation causes diffuse forces to exist far from the object, and crisp force vectors near the edges.

The GVF field points towards the object boundary when very near to the boundary, but varies smoothly over homogeneous image regions, extending to the image border (Fig. 9). The main advantage of the GVF field is that it can capture a snake from a long range. Thus, the problem of far initialisation can be alleviated.

The GVF is defined to be the vector field $G(x, y) = (u(x, y), v(x, y))$ that minimises the energy function:

$$E = \iint \left[\mu(u_x^2 + u_y^2 + v_x^2 + v_y^2) + |\nabla f|^2 |G - \nabla f|^2 \right] dx dy \quad (1)$$

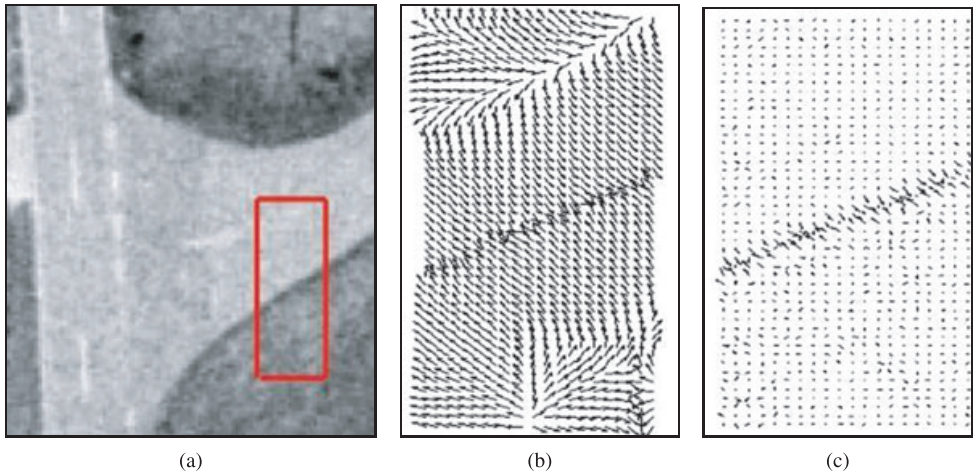


FIG. 9. (a) Test image with a selected box. (b) The GVF field. (c) The traditional force field of the box marked in (a).

where ∇f is the vector field computed from $f(x, y)$ having vectors pointing toward the edges. $f(x, y)$ is derived from the image having the property that it is larger near the image edges.

Regularisation parameter μ should be set according to the amount of noise present in the image. More noise requires a higher value of μ . Using the calculus of variations (Courant and Hilbert, 1953), the GVF can be found by solving the following Euler equations:

$$\begin{aligned} \mu \nabla^2 u - (u - f_x)(f_x^2 + f_y^2) &= 0 \\ \mu \nabla^2 v - (v - f_y)(f_x^2 + f_y^2) &= 0 \end{aligned} \quad (2)$$

where ∇^2 is the Laplacian operator. The ziplock snake that uses the GVF field as its external force field is called a GVF ziplock snake.

Let $V(s) = (x(s), y(s))$ be a parametric active contour in which s is the curve length and x and y are the image coordinates of the 2D curve. The internal snake energy is then defined as

$$E_{int}(V(s)) = \frac{1}{2} [\alpha(s)|V_s(s)|^2 + \beta(s)|V_{ss}(s)|^2] \quad (3)$$

where V_s and V_{ss} are the first and second derivatives of V with respect to s . The functions $\alpha(s)$ and $\beta(s)$ control the elasticity (the first term) and the rigidity (the second term) of the contour, respectively. The global energy has to be minimised

$$E = E_{int}(V(s)) + E_{img}(V(s)) \quad (4)$$

where $\alpha(s) = \alpha$ and $\beta(s) = \beta$ are constant. Minimising the energy function of equation (4) gives rise to the following Euler equations:

$$-\alpha V_{ss}(s) + \beta V_{ssss}(s) + \frac{\partial E_{img}(V(s))}{\partial V(s)} = 0 \quad (5)$$

where $V(s)$ stands for either $x(s)$ or $y(s)$, V_{ss} and V_{ssss} denote the second and fourth derivatives of V , respectively. Approximating the derivatives with finite differences and converting to vector notation with $V_i = (x_i, y_i)$, the Euler equations read

$$\alpha_i(V_i - V_{i-1}) - \alpha_{i+1}(V_{i+1} - V_i) + \beta_{i-1}[V_{i-2} - 2V_{i-1} + V_i] - 2\beta_i[V_{i-1} - 2V_i + V_{i+1}] + \beta_{i+1}[V_i - 2V_{i+1} + V_{i+2}] + G(u, v) = 0 \quad (6)$$

where $G(u, v)$ is the GVF vector field defined above. Equation (6) can be written in matrix form as

$$KV + G(u, v) = 0 \quad (7)$$

where K is a pentadiagonal matrix whose band is

$$[\beta_{i-1}; -\alpha_i - 2\beta_{i-1} - 2\beta_i; (\alpha_i + \alpha_{i+1}) + \beta_{i-1} + 4\beta_i + \beta_{i+1}; -\alpha_{i+1} - 2\beta_i - 2\beta_{i+1}; \beta_{i+1}].$$

Note that the first and last two rows of K must be modified to respect the boundary conditions because an open snake with fixed endpoints is used. Finally, the motion of the GVF ziplock snake can be written in the form (Kass et al., 1988):

$$V^{[t]} = (K + \gamma I)^{-1} * (\gamma V^{[t-1]} - \kappa G(u, v)|_{V^{[t-1]}}) \quad (8)$$

where γ stands for the viscosity factor (step size) determining the rate of convergence and t is the iteration index. The value of κ alters the strength of the external force.

With the GVF ziplock snake, limitations encountered with the original ziplock snake and the extensions of Laptev (1997) and Laptev et al. (2000) can be overcome. However, the proposed model might fail to detect the correct boundaries in the following cases:

- (1) High variation of curvature at the junction border resulting in too poor initialisation at some of its parts. Consequently the snakes become and remain straight (Fig. 10(a)).
- (2) The junction's central area lacks sufficient contrast with the surroundings causing the curve to converge to nearby features (Fig. 10(b)).

Using shape description parameters such as curvature computed from the snake vertices, another force was added to the GVF force field, the so-called balloon force, which lets the contour have a more dynamic behaviour (Cohen, 1991), thereby addressing the two problems described. This new force has the effect of inflating what was applied to the contour to localise

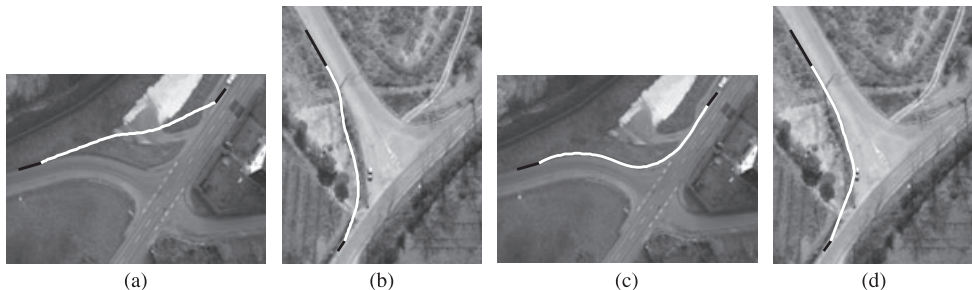


FIG. 10. (a) Optimisation result of the GVF snake in the presence of high variation of junction border curvature. In (b), the active contour cannot converge to the desired boundary due to the poor contrast. In (c) and (d), the improved results from adding balloon forces are displayed.

the concave part of the road junction. This force, which makes the contour act like a balloon, can be written as

$$F = k_1 \vec{n}(s) \tag{9}$$

where $\vec{n}(s)$ is the normal unitary vector of the curve at point $V(s)$ and k_1 is the amplitude of this force. Combining the GVF force field with the balloon force, equation (8) is modified:

$$V^{[t]} = (K + \gamma I)^{-1} * (\gamma V^{[t-1]} - \kappa G(u, v)|_{v^{[t-1]}} - k_1 \vec{n}(s)). \tag{10}$$

The balloon force is activated when the snake's passive and active parts are approximately straight, that is, their overall curvature, which is defined as the sum of the absolute curvatures along the curve, is below a threshold t_c . It is applied only on the passive part of the curve which is regarded as lying outside the junction's border, whereas the snake in its active parts is assumed to be on the right track. The improved results when the balloon force is applied are displayed in Figs. 10(c), (d).

Although the balloon force is applied on the passive part of the snake, active snake vertices that are close to the passive part are deformed accordingly to allow a smooth transition between the active and passive parts. This smoothness constraint is assured by the second term of the internal energy (rigidity). This characteristic is shown in Fig. 11 where a sequence illustrates successive steps in which the balloon force is applied.

The direction in which the balloon force is applied is towards the central area of the junction. The direction is computed by analysing the spatial direction of adjacent road sides in relation to each other.

Implementation Issues. In the implementation, $\alpha = 0.0001$ is chosen because the larger value forces the snake to become and then remain straight. By experiment, $\beta = 3$ was chosen to let the contour become smooth. To reduce the effect of disturbances, $\kappa = 0.1$ was used, that is, giving more weight to the internal than to the external force. The balloon force is applied when t_c has a value larger than 0.9, the amplitude of the force needs to be set smaller than the amplitude of the GVF (κ) so that edge points can stop the balloon force; a value of $k_1 = 0.025$ is used. Snake spacing refers to the distance between the sampled snake vertices. Denser snake vertices are more likely to be trapped and destabilised by small features such as road markings (Fig. 12(a)). Thus, convergence, assuming a small threshold to be achieved for the displacement from one iteration to the next, cannot always be reached. Conversely, when snake vertices are too sparse, concave object boundaries, as is often the case in road junctions, cannot be delineated correctly (Fig. 12(b)).

It is noticed that to some extent the latter problem can be solved by balloon forces. The snake spacing was set to 10 pixels (equivalent to 1 m) so that the movement of snake vertices is less likely to be blocked by trees, single cars and road markings. Likewise, the disturbing effects of the shadows cast by traffic lights and power lines are easily resolved. However, rows



FIG. 11. The effect of the balloon force in four successive steps. In (a), the balloon force is applied for the first time. In (c), a slight deformation of the bottom-right active part close to the passive part can be observed and in (d) both active and passive parts captured the junction boundary correctly.

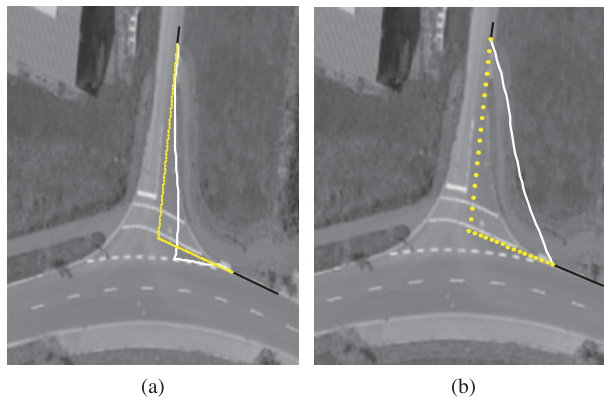


FIG. 12. Illustration of snake behaviour with different snake spacing settings. In (a), snake spacing is 2 pixels, which signifies dense initial vertices (yellow), and the convergence threshold is 1/200 pixel. Here, active contours are caught by road markings (white line). In (b), snake spacing is 14 pixels with the same convergence threshold. The optimised active contour cannot delineate the junction border, although the balloon force was applied.

of cars standing at traffic lights, and shadows from a row of buildings or trees might mislead the snake, resulting in convergence to wrong boundaries, because in such cases, a large number of vertices are trapped in the disturbing object. This situation affects the motion of neighbouring vertices and can eventually result in the delineation of the disturbing object boundaries or leakage into either the road junction area or the surroundings. Another problem which can occur frequently in roundabouts, but is less likely in simple and complex junctions, is that a close global initialisation cannot be provided when the angle between a pair of intersection lines is sharp ($<40^\circ$). As a result, the snake is unable to converge to the junction border. A closer global initialisation is supplied by decreasing the length of the intersection lines by half (Fig. 13).

In this approach, the force boundary is advanced by one vertex per iteration, when it can be verified that the motion of the corresponding active part has stabilised. Each active part is evaluated individually by testing whether the displacements in the x and y directions are less than a predefined threshold. Once two force boundaries meet, the viscosity factor is increased and the optimisation is repeated simultaneously on all vertices. This procedure often improves the quality of the final result at places where there is a small deviation from the object boundaries.

Intuitively, a lower value of γ is chosen when the process starts (because the curve is far from the solution), and a larger value when the snake is close to the contour (Berger and Mohr, 1990). Fig. 14 illustrates the evolution of the snake including intermediate results.

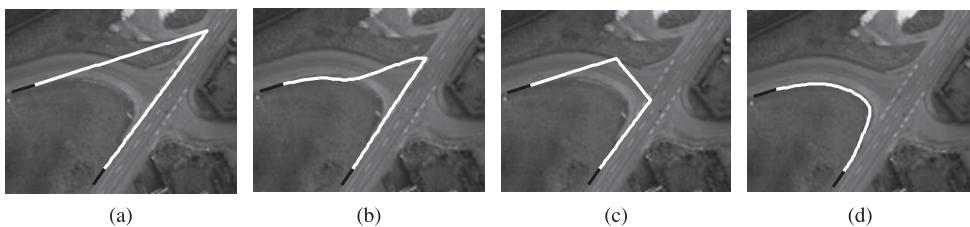


FIG. 13. (a) The intersection lines when their intersection angle is sharp (35°) and (c) the intersection lines whose lengths were modified. In (b) and (d), the results of the snake optimisation for (a) and (c) are displayed, respectively.

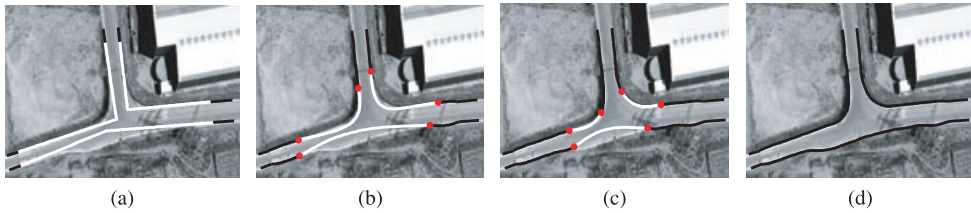


FIG. 14. Snake evolution. (a) White lines depict initial curves and black lines depict the extracted road arms. (b), (c) Intermediate results in which force boundaries are depicted as red points. (d) The final result.

RESULT AND EVALUATION

For the experiments, black-and-white aerial ortho-imagery was used, derived from Digital Mapping Camera (DMC) images with a ground resolution of 0.1 m. The images were taken from rural and suburban areas in Germany. Because the number of junctions in one scene is generally low, junctions are selected from a large number of images. As well as the images, external vector data is taken from the Authoritative Topographic Cartographic Information System of Germany (ATKIS). The content of ATKIS is approximately equivalent to topographic maps at 1:25 000 scale. In this database, roads are modelled as linear objects and junctions as point objects.

The contour-following property of ziplock snakes, when combined with the large capture range capability of the GVF force field and the non-convex object detection property of balloon forces, enables delineation of road junctions in high-resolution aerial ortho-imagery. To demonstrate this potential, the proposed approach was tested on 40 road junction samples with the same set of control parameters for the balloon-guided GVF ziplock snake method. The parameter setting for the road model is illustrated in Table I. Some selected results are given to prove its capabilities (Fig. 15). The approach can deal with disturbances caused by road markings and shadows, as can be seen in the top-left sample where the effect of shadows from the truck, street lights and the tree are removed and, in the top-middle and top-right images, the stop and warning lines do not affect the quality of the extraction. In the bottom-middle example, strong crosswalks connected together by a secondary road are also overcome. In the bottom-left sample, junction borders at the top and bottom have a very high curvature resulting in an initialisation far from the correct positions. There is a sharp contrast between the junction area and the surroundings. However, the central area of the junction contains two regions with different radiometric characteristics such that the region on the top is brighter than that on the bottom. As a result, it is hard to pull the initial contour back towards the junction border. The snake method is able to handle such a situation. Furthermore, the snake curve can pass through a large shadow region and successfully localises the true boundary as is shown in the bottom-right image.

In order to evaluate the performance of the approach, the extracted junctions were compared to manually plotted road junction areas used as reference data. The comparison was carried out by matching the extracted *road borders*, which resulted from connecting the junction border to the associated road sides, to the reference data using the so-called *buffer method* (Heipke et al., 1998). Although the buffer width can be defined using the required accuracy of ATKIS, which for a road object is defined as 3 m, it was decided to set the buffer width within the range of 0.5 to 3 m, that is, 5 to 30 pixels in concert with the image resolution of 0.1 m. This allows assessment of the relevance of the approach for practical applications that demand varying degrees of accuracy. A smaller value of the buffer width is chosen for an



FIG. 15. Road junction extraction results. Image samples represent scenes that contain varying degrees of complexity including disturbances.

application that requires more accurate extraction results. An extracted road border is assumed to be correct if the maximum distance between the extracted road border and its corresponding reference does not exceed the buffer width. Based on these assumptions the following quality measures were used:

Completeness: the ratio of the number of correctly extracted road borders to the reference number.

Geometrical accuracy: the average distance between the correctly extracted road border and the corresponding reference road border, which is expressed as the rms value falling within the range of [0, buffer width].

Table II shows the evaluation results computed with different buffer width values. From the buffer width value of 0.5 to 3 m, the completeness of the road border extraction has increased, implying that the results are more complete for higher buffer width values. The geometric accuracy increases are inversely proportional to the buffer width value so that results obtained with a value of 0.5 are more accurate than those obtained with a larger buffer width.

TABLE II. Evaluation results for 40 road junctions.

	<i>Buffer width (m)</i>			
	<i>0.5</i>	<i>1</i>	<i>2</i>	<i>3</i>
Reference number of road borders	143	143	143	143
Completeness	51%	61%	73%	78%
Geometric accuracy (m)	0.31	0.41	0.54	0.59

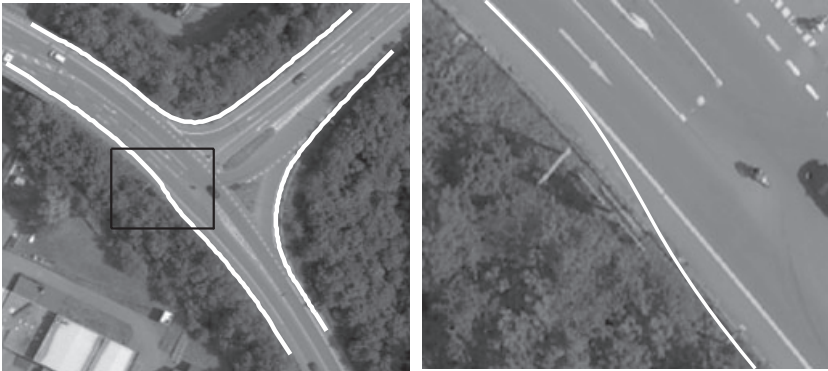


FIG. 16. Incorrectly extracted road border. Marked box in the left image shows the area where inconsistency occurs. This area is displayed in detail in the right image.

For the buffer width value 0.5 m, the completeness is rather low. The reason is that a slight deviation of the extraction results from the true boundaries exceeding the buffer width frequently occurs due to disturbances and sometimes also due to road markings. One example describing such a problem is given in the top-right image in Fig. 15. In this example, the top-left road border has converged slightly inside the junction area. The deviation from the junction border is less than 1 m and thus shows up as an error for the smallest buffer width. For the buffer widths of 2 and 3 m, significantly higher quantities of completeness have been achieved, which points to the validity of the present approach for many practical applications.

Where one of the associated road sides from two neighbouring road arms is located on the road side and another on a road marking, inconsistency occurs. In the present approach, this inconsistency cannot be overcome (Fig. 16). In this example, the right part of the road border has been extracted correctly, but the left part lies somewhat within the road. The same problem can occur when in one of the neighbouring roads, road sides cannot be extracted because of occlusions or disturbances. These problems can only be addressed by a more sophisticated road model including width constraints and disturbing objects.

CONCLUSION AND OUTLOOK

In this paper, a new approach to extracting road junctions from high-resolution aerial ortho-images is proposed. It comprises a new snake-based method that enables the delineation of the junction border making use of an existing geospatial database. The geospatial database gives a rough idea of the junction by supplying information on geometric, topological and radiometric characteristics of the junction. The derived information is used to guide the extraction of road arms. Extracted road arms help to provide a close initialisation for the snake. The GVF external force field was integrated into the traditional ziplock snake to increase the snake's capture range and added the balloon force to overcome both the curvature variation along the junction border and poor results caused by lack of sufficient contrast between the central area of the junction and the surroundings. Furthermore, various kinds of disturbances were resolved by using a strong internal force and by providing a global initialisation. The results of applying this approach to 40 samples are shown and a quantitative evaluation of the results using a range of buffer width values is presented.

It has been shown that active contours can be used to delineate complex man-made objects if the shape information of the object is incorporated into the snake evolution. Furthermore, it was found that a strong internal energy combined with a dense external force field and a proper initialisation is able to overcome various kinds of disturbances.

The current approach is developed to delineate simple road junctions in rural and suburban areas. The authors believe that it can be extended to urban areas provided that vehicles are taken into account in the road arm model. In urban areas, groups of vehicles are usually present on the intersecting roads in the area close to a junction, thus causing the road arm extraction process to break down.

The next goal will be the extraction of complex junctions. Traffic islands need to be modelled and detected, as complex junctions include a varying number of these small islands. The extraction of roundabouts is another goal that will be pursued in future research as roundabouts are regarded as a subclass of complex junctions. Furthermore, investigations into the possibility of using the current snake model in images with different ground resolutions will be carried out.

REFERENCES

- BARSI, A., HEIPKE, C. and WILLRICH, F., 2002. Junction extraction by artificial neural network system—JEANS. *International Archives of Photogrammetry and Remote Sensing*, 34(3B): 18–21.
- BERGER, M.-O. and MOHR, R. 1990. Towards autonomy in active contour models. *Proceedings, 10th International Conference on Pattern Recognition*, 1: 847–851.
- BOICHIS, N., COCQUEREZ, J.-P. and AIRAULT, S. 1998. A top down strategy for simple crossroads extraction. *International Archives of Photogrammetry and Remote Sensing*, 32(2/1): 19–26.
- BOICHIS, N., VIGLINO, J.-M. and COCQUEREZ, J.-P., 2000. Knowledge based system for the automatic extraction of road intersections from aerial images. *International Archives of Photogrammetry and Remote Sensing*, 33(B3): 27–34.
- COHEN, L. D., 1991. On active contour models and balloons. *Computer Vision, Graphics, and Image Processing: Image Understanding*, 53(2): 211–218.
- COURANT, R. and HILBERT, D., 1953. *Methods of Mathematical Physics*. Volume 1. Wiley-Interscience, New York. 575 pages.
- GAUTAMA, S., GOEMAN, W. and D'HAeyer, J., 2004. Robust detection of road junctions in VHR images using an improved ridge detector. *International Archives of Photogrammetry, Remote Sensing and Spatial Information Sciences*, 35(B3): 815–819.
- GERKE, M., 2006. *Automatic quality assessment of road databases using remotely sensed imagery*. Wissenschaftliche Arbeiten der Fachrichtung Geodäsie und Geoinformatik der Leibniz Universität Hannover 261, and Deutsche Geodätische Kommission, Reihe C, No. 599. Beck Verlag München. 105 pages.
- GUNST, M. DE and VOSSELMAN, G., 1997. A semantic road model for aerial image interpretation. In *Semantic Modeling for the Acquisition of Topographic Information from Images and Maps, SMATI 97* (Eds. W. Förstner & L. Plümer). Birkhäuser Verlag, Basel. 227 pages: 107–122.
- HEIPKE, C., STEGER, C. and MULTHAMMER, R., 1995. A hierarchical approach to automatic road extraction from aerial imagery. *Integrating Photogrammetric Techniques with Scene Analysis and Machine Vision II, SPIE* 2486: 222–231.
- HEIPKE, C., MAYER, H., WIEDEMANN, C. and JAMET, O., 1998. External evaluation of automatically extracted road axes. *Photogrammetrie Fernerkundung Geoinformation*, 2/1998: 81–94.
- HINZ, S., BAUMGARTNER, A., STEGER, C., MAYER, H., ECKSTEIN, W., EBNER, H. and RADIG, B., 1999. Road extraction in rural and urban areas. *Semantic Modeling for the Acquisition of Topographic Information from Images and Maps, SMATI 99*, München: 7–27.
- KASS, M., WITKIN, A. and TERZOPOULOS, D., 1988. Snakes: active contour models. *International Journal of Computer Vision*, 1(4): 321–331.
- LAPTEV, I., 1997. *Road extraction based on line extraction and snakes*. Master's thesis, Computational Vision and Active Perception Laboratory (CVAP), Royal Institute of Technology (KTH), Stockholm, Sweden. 67 pages.
- LAPTEV, I., MAYER, H., LINDBERG, T., ECKSTEIN, W., STEGER, C. and BAUMGARTNER, A., 2000. Automatic extraction of roads from aerial images based on scale space and snakes. *Machine Vision and Applications*, 12(1): 23–31.

- MAYER, H., LAPTEV, I. and BAUMGARTNER, A., 1998. Multi-scale and snakes for automatic road extraction. *Lecture Notes in Computer Science*, 1406: 720–733.
- NEUENSCHWANDER, W. M., FUA, P., IVERSON, L., SZÉKELY, G. and KÜBLER, O., 1997. Ziplock snakes. *International Journal of Computer Vision*, 25(3): 191–201.
- RAVANBAKHSI, M., HEIPKE, C. and PAKZAD, K., 2007. Road junction extraction from high resolution aerial images. *International Archives of Photogrammetry, Remote Sensing and Spatial Information Sciences*, 36(3/W49B): 131–137.
- STEGE, C., 1998. An unbiased detector of curvilinear structures. *IEEE Transactions on Pattern Analysis and Machine Intelligence*, 20(2): 113–125.
- WANG, J. and LI, X., 2003. Guiding ziplock snakes with a priori information. *IEEE Transactions on Image Processing*, 12(2): 176–185.
- WIEDEMANN, C., 2002. Improvement of road crossing extraction and external evaluation of the extraction results. *International Archives of Photogrammetry and Remote Sensing*, 34(3B): 297–300.
- XU, C. and PRINCE, J. L., 1997. Gradient vector flow: a new external force for snakes. *Proceedings of IEEE Conference on Computer Vision and Pattern Recognition (CVPR)*: 66–71.
- ZHANG, C., 2003. *Updating of cartographic road databases by images analysis*. Ph.D. thesis. Report No. 79, Institute of Geodesy and Photogrammetry, ETH Zurich, Switzerland. 188 pages.

Résumé

Les carrefours routiers sont des composantes importantes d'un réseau routier. Ils ne sont cependant habituellement pas explicitement modélisés dans les approches existantes d'extraction de routes. Dans ce travail, nous modélisons en détail les intersections de routes comme des objets surfaciques et proposons une solution pour leur extraction automatique grâce à l'utilisation d'une base de données géospatiale existante. Des contraintes a priori issues d'une base de données topographique géospatiale sont utilisées pour faciliter la détection. Nous proposons une nouvelle approche, fondée sur des contours actifs (snakes). Elle utilise le modèle «ziplock snake» et son énergie externe est une combinaison d'une force de flux du vecteur du gradient (GVF) et d'une force ballon afin de tracer les contours des carrefours. Les résultats de l'extraction des axes routiers fournissent des conditions de frontières fixes au contour actif proposé. L'approche a été testée avec des ortho-images aériennes panchromatiques de résolution 0,1 m issues de la caméra numérique DMC sur des zones semi-urbaines et rurales. Les résultats obtenus montrent la validité de la solution.

Zusammenfassung

Straßenkreuzungen sind wichtige Komponenten eines Straßennetzes. Sie sind aber in vorhandenen Straßenextraktionsansätzen in der Regel nicht explizit modelliert. In unseren Arbeiten modellieren wir Kreuzungen im Detail als Flächenobjekte und schlagen einen Ansatz für ihre automatische Extraktion unter Verwendung einer Geodatenbank vor. Die Informationen aus der topographischen Datenbank werden als Vorwissen genutzt, um die Extraktion zu erleichtern. Wir schlagen ein neuartiges Modell vor, welches das „Ziplock Snake“-Konzept verwendet und dessen äußere Energie eine Kombination aus Gradient Vector Flow (GVF) und Balloon Forces darstellt. Mit Hilfe des „Snake Model“ werden die Kreuzungsgrenzen extrahiert. Die Ergebnisse der vorangegangenen Straßenextraktion liefern die Randbedingungen für das vorgeschlagene „Snake Model“. Der Ansatz wurde unter Verwendung monochromer Luftbilder aus suburbanen und ländlichen Gebieten getestet, die mit einer Digital Mapping Camera (DMC) mit einer Bodenauflösung von

0,1 m aufgenommen wurden. Die Ergebnisse demonstrieren die Anwendbarkeit unseres Ansatzes.

Resumen

Las intersecciones son un componente muy importante de una red viaria. Sin embargo, normalmente los métodos de extracción de carreteras existentes no las modelan explícitamente. En esta investigación se modelan con detalle las intersecciones como objetos superficiales y se propone un procedimiento para su extracción automática mediante la utilización de una base de datos geospacial preexistente. Para facilitar la extracción se utiliza la información previa obtenida de una base de datos topográfica. El nuevo procedimiento se basa en curvas activas (snakes) y se apoya en el concepto de las curvas activas selladas (ziplock snakes) cuya fuerza externa es una combinación de la fuerza de flujo del vector del gradiente y de una fuerza de globo para delinear el contorno de la intersección. El resultado de la extracción de los tramos crea las condiciones límite para la curva activa propuesta. El método se ensayó usando ortoimágenes en blanco y negro de 0,1 m de resolución obtenidas con una Digital Mapping Camera (DMC) en áreas suburbanas y rurales. Los resultados obtenidos demuestran la validez del método.